Simple temperature insensitive fiber Bragg grating based tilt sensor with enhanced tunability

R. Aneesh,[1] Meeth Maharana,[1] Pathi Munendhar,[1] H. Y. Tam,[2] and Sunil K. Khijwania[1,*]

[1]Department of Physics, Indian Institute of Technology Guwahati, Guwahati, Assam 781039, India

[2]Photonic Research Centre, The Hong Kong Polytechnic University Kowloon, Hong Kong SAR

*Corresponding author: skhijwania@iitg.ernet.in

Received 18 March 2011; revised 25 July 2011; accepted 29 July 2011;
posted 1 August 2011 (Doc. ID 144305); published 16 August 2011

A design for an all-optical temperature insensitive fiber Bragg grating (FBG) based tilt sensor is reported. The sensor is capable of measuring the magnitude as well as the direction of inclination from the horizontal with a complete reversible response over the designed dynamic range of ±45°. The most important feature of the reported sensor is its inherent enhanced tuning capability for its sensitivity. An excellent sensitivity of the order of ~0.0626 nm/° that can further be tuned is observed for the sensor. Experimental results show that a tilt angle resolution better than 0.008° with a tilt accuracy of ~ ± 0.36° was achieved. © 2011 Optical Society of America

OCIS codes: 060.2370, 060.3735.

1. Introduction

With the advancement of fiber Bragg grating (FBG) technology and its well-known strain sensitivity, lots of potential sensor applications have been explored over the last decade [1]. Numerous attempts have been made in order to map various parameters of interest. e.g. pressure [2], acceleration [3,4], torsion [5], flow [6], etc. in terms of strain. The reason for such a trend is, FBG based all-optical sensor is advantageous in terms of the fact that it includes, but is not limited to, the merits of fiber optic sensors. Inclination or tilt angle measurement is another important parameter in terms of civil, mechanical, instrumentation, robotics, and aeronautical engineering applications. Its measurement employing laser technology has an advantage of large dynamic range [7]. However, such methodologies are impractical for real-field applications, owing to their bulk/complicated and expensive configurations. Recently, a few FBG based attempts have been made for inclination/tilt measurement [8–14]. Though a very high resolution was achieved [8], the performance in these studies was limited by the design constraints such as a cantilever based pendulum suspension mechanism resulting in friction and corresponding instabilities in [8,9,11] and predeflections of steel flakes with a complicated pendulum suspension mechanism in [9]. All these designs relied on the rotation of the pendulum while applying the tilt and hence suffered from the unwanted and inherent mechanical frictions of the joints during the rotation. In [10], a design strategy based on single FBG was proposed. Nevertheless, the sensitivity in all the reported sensors was limited. He *et al.* in [12] reported a tilt sensor based on three FBGs in series on a single fiber making an inverted pyramidal structure with three fiber arms and a mass (bob) suspended from the vertex. A very high-sensitivity was observed. However, retrieval of the tilt was based on a very intricate mathematical analysis. Ni *et al.* [13] reported another tilt sensor based on four FBGs in series on a single fiber making an inverted pyramidal structure with four fiber arms and a mass (bob) suspended from the vertex. Nevertheless, stability of the sensor and the cross-sensitivity to unwanted perturbations in both the designs are important issues. As the mass is hanged directly to the fiber loop, any unwanted add-on oscillation is expected to lead to a random vibration/oscillation of the fiber-mass pendulum system of both the sensor designs in [12,13]. This is

0003-6935/11/25E172-05$15.00/0
© 2011 Optical Society of America

bound to give measurement errors and will make these sensors highly unstable. Also, there is a possibility of slacking of one fiber arm in the plane of inclination during the tilt. Au *et al.* [14] reported another tilt sensor based on four FBGs in the horizontal plane with a response linearly tunable in proportion of the mass of the used bob.

In this paper, we report a simple, stable, and modified FBG based tilt sensor having inherent enhanced tuning capability for its sensitivity. The design strategy intrinsically negates the possibility of noise/error due to any add-on unwanted perturbations. The proposed sensor is also free from any mechanical joints/inherent frictions and theoretically capable of monitoring tilt/inclination from horizontal in a dynamic range of ±45°. Enhanced (nonlinear) tunability is achieved by varying just one sensor parameter, namely the mass of the bob. Experiments were carried out over the range of only ±10°, owing to the limitation of the available tilt stage in the laboratory. The design of the sensor allows a rigorous and active (in-line) tuning of the applied prestrain to the grating for performance optimization. Sensing strategy is based on decoding the inclination/tilt angle information from the peak wavelength separation between two FBGs. This makes the diagnosing procedure completely temperature independent. Experimental results show that a tilt angle resolution better than 0.0064°, tilt accuracy of ±0.3°, and the sensitivity of the order of ∼0.0626 nm/° was achieved.

2. Sensor Design and Principle

Two square aluminum plates of dimension $5 \times 5 \times 1\,\mathrm{cm}^3$ were joined by four identical vertical brass rods of diameter 0.6 cm (Fig. 1). A rectangular prism of dimension $1.7 \times 0.8 \times 1\,\mathrm{cm}^3$ was removed from the center of the four edges of the top plate. These removed rectangular prisms were replaced by four

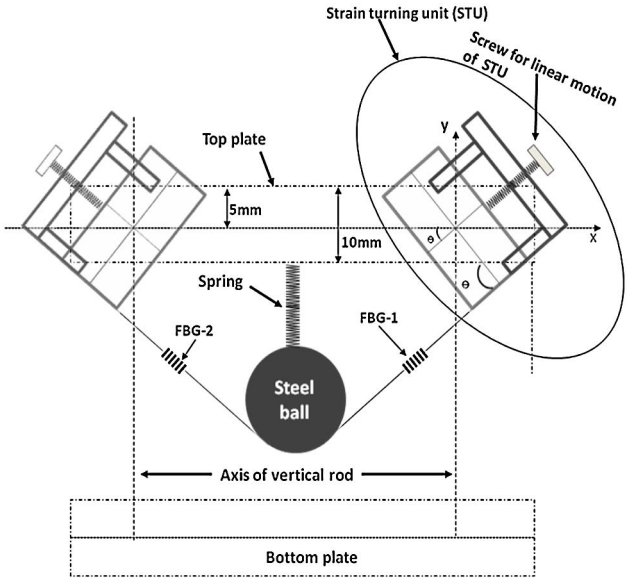

Fig. 1. Schematic diagram of prestraining FBGs using STU.

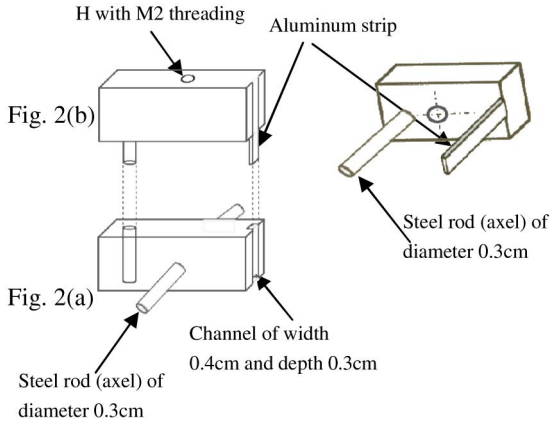

Fig. 2. (a) Part A of STU; (b) part B of STU with two side image.

specially designed small units, termed as strain tuning units (STUs) (see encircled part of Fig. 1 for schematics of STU). Each STU consists of two parts, namely A and B (Fig. 2). Part A, termed as the base plate, is an aluminum rectangular prism of dimension $1.59 \times 0.8 \times 1\,\mathrm{cm}^3$, with a steel axle through the center of the two opposite vertical faces of the prism. On one side of this prism, a vertical channel of width 0.4 cm and depth 0.3 cm was made. Close to the opposite side of this prism (0.35 cm from the edge), a hole of diameter 0.3 cm was drilled [Fig. 2(a)]. Part B is an aluminum rectangular prism of dimension $1.7 \times 0.8 \times 1\,\mathrm{cm}^3$. It has an aluminum strip of dimension $1 \times 0.4 \times 0.3\,\mathrm{cm}^3$ on one side. Close to the opposite side of this prism (at distance 0.46 cm), a steel rod of diameter 0.3 cm was fixed [Fig. 2(b)]. At the center of this prism, a hole (H) having M2 threading was made and a M2 screw was fixed in it. Part B was fixed onto part A. While turning the M2 screw, part B moved linearly against the base plate irrespective of the base plate's orientation (Fig. 3). The axel of part A was fixed at the middle of the width of the top plate (Fig. 4). Part A, and, hence STU, were free to rotate within 0–90°. Nevertheless, part A was kept static at a given orientation with the help of two adjusting screws (Fig. 4). Thus, each STU was capable of moving linearly at a predetermined angle and provided a fine strain tuning mechanism. From the center of the top plate, a steel bob was hanged through a spring of optimized spring constant. Four FBGs were written

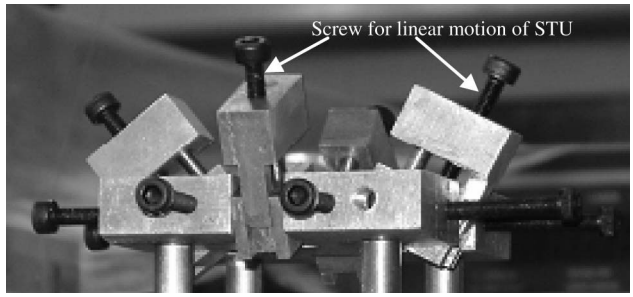

Fig. 3. Linear motion of part A of STU against part B using M2 screw.

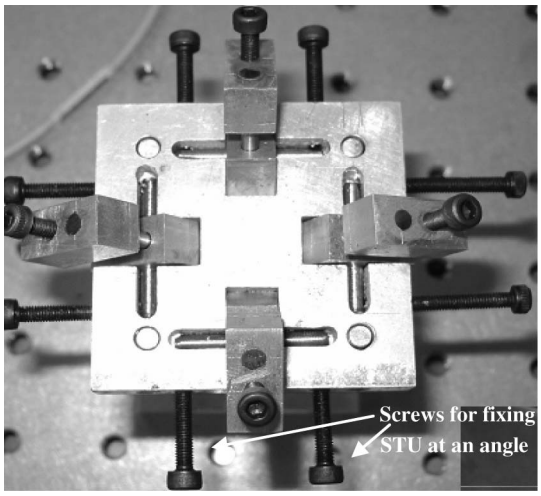

Fig. 4. Top plate with STUs fixed on it.

onto a single fiber such that the distance between FBG1 (λ_1) and FBG2 (λ_2) as well as FBG3 (λ_3) and FBG4 (λ_4) were kept identical. The fiber carrying four FBGs was glued at the center of the first STU, then to the bottom of the bob, then to the opposite, i.e., the third STU; then to the second STU, and via the bottom of the bob to the opposite, i.e., fourth STU; thus making two crossing triangular/inclined fiber arms each having a curved vertex at the bottom of the bob. In this arrangement, FBGs rested at the middle of the fiber joining STU and the bottom of the bob. The spring was maintained to its natural length by prestraining each fiber arm equally along the crossed and inclined directions through STUs. The center of gravity (CG) of the bob was ensured to be at the vertical line (longitudinal axis) joining the center of the top and the bottom plates. It is important to mention that the role of the spring was to give the stability to the proposed sensor. In the absence of the spring, the bob is bound to rotate with respect to its bottom point where fibers are glued while applying tilt (say in x-z plane). This will lead to the slacking of the fiber arms and the random strain distribution. Further, its CG will also get displaced from the longitudinal axis of the sensor. Owing to this, the angle θ made by FBG1 and FBG2 from the top plate (Fig. 1) will no longer remain the same and will change to two different angles, say α and β. These angles will vary slightly with the inclination angle in different ratios. It is the same with the case in the y-z plane. Another two different angles, say α' and β', will be induced and vary with the inclination angle. In an ideal situation, deviation from θ to these angles should be very small and negligible. Further, sensor performance critically depends on the spring's characteristics. Springs of various spring constants were considered in optimizing the sensor performance. A spring with a low spring constant resulted in the deformation of the four fiber arms carrying FBGs while applying tilt. With such springs, it was difficult to keep the CG of the bob in the longitudinal axis of the sensor, to avoid the rotation of the bob and to avoid the slacking of fiber arms during the application of the tilt. Further, the sensor with such a spring (low spring constant) was observed to be unstable with the spring-mass-fiber system vibrating in response to any unwanted add-on perturbation and thus modulating the sensor characteristics with unwanted noise. Increasing the spring constant resulted in a better stability and less deformation of the sensor. A spring with a particular higher value of the spring constant that almost negated the deformation (rotation of the bob, deviation of CG from the sensor's longitudinal axis, slacking of fiber arms, etc.) was used in the final sensor design. The total dimension of the sensor was $5 \times 5 \times 8\,\mathrm{cm}^3$. A photograph of the developed sensor is shown in Fig. 5.

When the sensor is inclined by an angle ϕ, say, in the y-z plane, keeping the inclination in the x-z plane zero, the strain in the gratings gets redistributed and the corresponding wavelength shift difference is given by

$$\Delta(\lambda_2 - \lambda_1) = \frac{(1 - P_e)mg\lambda_1 \sin\phi}{AE\cos\theta}, \tag{1}$$

and

$$\Delta(\lambda_4 - \lambda_3) = 0. \tag{2}$$

In the same way, when the sensor is inclined by an angle ϕ, say, in the x-z plane, keeping the inclination in the y-z plane zero, the strain in the gratings gets redistributed and the corresponding wavelength shift difference is given by

$$\Delta(\lambda_4 - \lambda_3) = \frac{(1 - P_e)mg\lambda_3 \sin\phi}{AE\cos\theta}, \tag{3}$$

and

$$\Delta(\lambda_2 - \lambda_1) = 0. \tag{4}$$

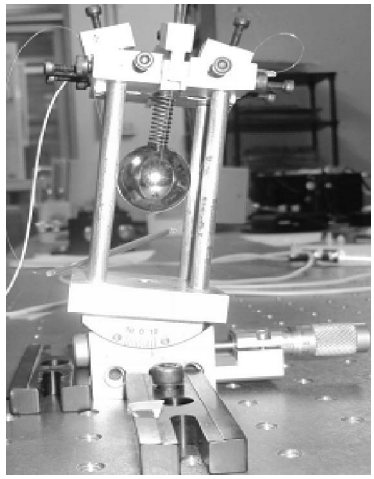

Fig. 5. Proposed FBG based tilt sensor.

Here, m is the mass of the bob, g is the acceleration due to gravity, P_e is the photoelastic constant of the fiber, A is the area of cross-section of the fiber, E is the Young's modulus of the material of the fiber, and θ is the angle made by the fiber arms from the horizontal. Equations (1) and (3) show that the wavelength separations are linearly proportional to $\sin\phi$. Further, as the temperature-change during the experiment shifts each FBG's wavelength in the same direction, measuring the tilt angle through the wavelength separation between the two FBGs overcomes the problem of temperature cross-talk in the final measurement, thus making the sensor temperature independent. The most striking feature of the proposed sensor is its inherent enhanced (nonlinear) tuning capability for its sensitivity. This can be understood by analyzing Eqs. (1) and (3). It can be observed that, instead of one, there are two factors influencing the sensitivity: namely m and $\cos\theta$. As m increases, the size of the bob and hence θ increases. The increase of θ leads to a nonlinear increase of $1/\cos\theta$. Thus, the linear increase in m and the nonlinear increase in $1/\cos\theta$ multiplied together leads to a manifold increase in the sensor's sensitivity. It is worth mentioning that this enhanced sensitivity tuning is realized by changing only one parameter, namely the mass of the bob m. This is in contrast to [12–14], where an increase in mass results in a linearly proportional increase in the sensitivity. One needs to change other sensor parameters, e.g., fiber length or the dimension of the top plate in [12,13].

3. Experiment and Results

Four FBGs were written onto a hydrogen-loaded single-mode fiber using phase-mask method. The parameters of the fiber used are $E = 7.27 \times 10^{10}$ N/m^2, $A = 1.2266 \times 10^{-8}$ m^2, and $P_e = 0.22$. Also, the peak reflection wavelengths of FBGs are 1544.56 nm(λ_1), 1536.75 nm(λ_2), 1559.34 nm(λ_3), and 1571.05 nm(λ_4). The fiber was glued at two opposite STUs through the bottom of the bob (having mass 67 g) as explained in the previous section. The four FBGs rested at the center of each arm. These gratings were prestrained by a predetermined value through the STUs. The spring maintained its natural length with the center of the bob passing through the line joining the center of the top and bottom square plates. The sensor was mounted on the available tilt stage (goniometer), which had a provision to turn the sensor within ±10° range only. These were the laboratory constraints. It is important to mention that the sensor is not limited to a maximum tilt of ±10°, rather it is designed for a ±45° applied tilt. To carry out the experiment, the sensor was first tilted in the y-z plane and the wavelength shifts for four FBGs corresponding to different values of the tilt angle (ϕ) were recorded using an interrogator. The tilt angle was varied from −10° to 10° (forward) and then back to −10° (reverse) in a suitable minimum amount of steps allowed by the goniometer. Experimentally observed $\Delta(\lambda_2 - \lambda_1)$ for forward and reverse tilt angles are shown in Fig. 6 (mass-1, triangle for forward, and tilted square for reverse tilt). As can be observed from Fig. 6, the sensor response is linear for the forward as well as the reverse tilt. The measured sensitivities for forward and reverse directions are found to be 0.0123 nm/° and 0.0122 nm/°, respectively, showing a highly reversible nature of the sensor. It is important to mention that $\Delta(\lambda_4 - \lambda_3)$ was found to be zero in this case as predicted by Eq. (2). A similar response was observed when a tilt was applied in the x-z plane for both forward and reverse directions. Further, the maximum discrepancy is observed to be less than ±0.0069 nm, with a corresponding angular uncertainty of ±0.5609° for both forward and reverse directions in both the planes. The resolution of the sensor completely depends on the resolution of the interrogating device. The wavelength resolution of 0.5 pm of the interrogator resulted in the angular resolution of 0.0407° for the sensor.

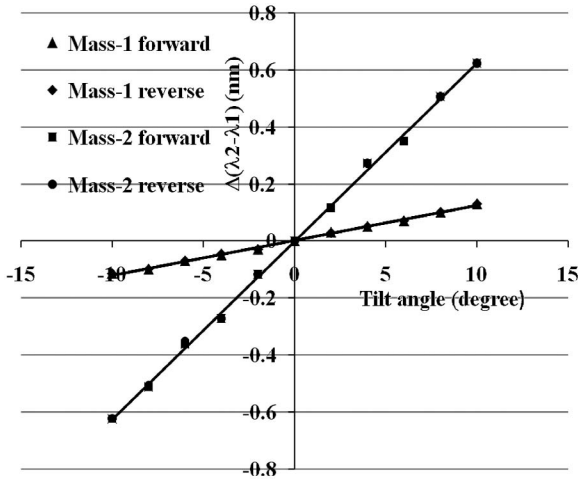

Fig. 6. Experimentally observed sensor responses with two different masses.

As can be observed from the design principal of the sensor [Eq. (1) or (3)],the sensitivity can be increased manifold by simply increasing the mass of the bob. Hence, in the next step, in order to see the effect of mass on sensor performance, another senor was developed by replacing the existing bob of mass 67 g with another bob of mass 110.3 g. The experiment was repeated for the sensor comprising the new bob of higher mass. The experimentally observed sensor responses for forward and reverse directions are shown in Fig. 6 (mass-2, square, and circular points). As can be observed from the figure, the sensor response is linear for forward as well as reverse directions with corresponding sensitivities of 0.0626 nm/° and 0.0624 nm/°, respectively. Importantly, the increase in the mass of the bob from 67 g (mass-1) to 110 g (mass-2), which is 1.64 times increase, results in a 5.1 times increase in the sensitivity. Such a manifold sensitivity enhancing/tuning capability is achieved for the first time to the best of the author's knowledge. Further in comparison to the

Table 1. Comparison of the Sensor Response

Author	Mass of bob (g)	Sensitivity (nm/°)	Accuracy	Resolution	Dynamic range
Guan *et al.* [8]	344	0.0752	±0.1°	0.007°	−09° to +03°
Chen *et al.* [10]	357	0.0600	±0.167°	0.0067°	−15° to +15°
Bao *et al.* [11]	500	0.096	±0.2°	0.013°	−40° to +40°
He *et al.* [12]	200	0.192	±0.1°	0.005°	−12° to +12°
Ni *et al.* [13]	100	0.0537	-	0.009°	−10° to +10°
Au *et al.* [14]	170	0.0395	±0.051°	0.013°	−07° to +07°
Reported sensor	110	0.0626	±0.36°	0.008°	−10° to +10°

resolution of 0.0407° in the case of sensor with mass-1, a resolution of 0.0080° was observed for the sensor with mass-2., The maximum discrepancy and corresponding angular uncertainty were observed to be ±0.0231 and ±0.3403°, respectively. The accuracy of the tilt angle measurement is thus observed to be $\sim \pm 0.36°$. Next, we compared the performance characteristics of the proposed sensor with the other FBG based tilt sensors reported in the literature. Table 1 lists a few important features of these sensors for comparison. As can be observed from the Table 1, the highest sensitivity of 0.192 nm/° was reported by He *et al.* [12] within the dynamic range of −12° to +12°. However, the mass of the bob used in [12] was 200 g, which is 1.8 times higher than the mass (mass-2) used in the reported sensor. If the mass in the present sensor is increased to the mass used by [12], and if we still assume a 5.1 times increase in the sensitivity (which actually corresponds to 1.64 times increase in mass), the expected sensitivity would be of the order of 0.319 nm/°. This is much higher than the reported sensitivity in [12]. It is worth mentioning again that the measured tilt range for the proposed sensor was limited to the maximum tilt span (±10°) of the available goniometer in the laboratory and we could not execute experiments to the designed range of ±45°.

4. Conclusion

An all-optical fiber tilt sensor based on four FBGs is reported. This sensor is free from the design constraints of other reported sensors. The proposed sensor is capable of measuring the magnitude as well as the direction of the inclination from the horizontal direction. The sensor has provision to increase the sensitivity manifold by simply increasing the mass of the bob. The sensor response is investigated with two different masses in a tilt measurement range of −10°–10° (limited by the range of available goniometer). The sensor is designed and capable of measuring tilt in the dynamic range of −45° to +45°. For both masses, the sensor responses are observed to be linear and highly reversible. With higher mass, measured sensitivity is found to be 0.0626 nm/° for forward direction and 0.0624 nm/° for reverse direction in the *y*-*z* plane with tilt angle accuracy of ±0.36° and resolution of 0.008°. An identical response was observed in the *x*-z plane also. The major limitation associated with a FBG based sensor is the temperature cross-sensitivity. However, as the developed sensor measures tilt angle by measuring the difference in wavelength shifts of two FBGs, it is free from temperature cross-sensitivity. Hence, it can be used for real-field industrial/engineering applications.

References

1. A. D. Kersey, M. A. Davis, H. J. Patrick, M. LeBlanc, K. P. Koo, C. G. Askins, M. A. Putnam, and E. J. Friebele, "Fiber Bragg grating sensors," J. Lightwave Technol. **15**, 1442–1463 (1997).
2. J. Yang, Y. Zhao, B. J. Peng, and X. Wan X, "Temperature-compensated high pressure FBG sensor with a bulk-modulus and self-demodulation method," Sens. Actuators A, Phys. **118**, 254–258 (2005).
3. M. D. Todd, G. A. Johnson, B. A. Althouse, and S. T. Vohra, "Flexural beam-based fiber Bragg grating accelerometers," IEEE Photon. Technol. Lett. **10**, 1605–1607 (1998).
4. T. A. Berkoff and A. D. Kersey, "Experimental demonstration of a fiber Bragg grating accelerometer," IEEE Photon. Technol. Lett. **8**, 1677–1679 (1996).
5. X. G. Tian and X. M. Tao, "Torsion measurement using fiber Bragg grating sensors," Appl. Opt. **41**, 248–253 (2001).
6. J. Lim, Q. P. Yang, B. E. Jones, and P. R. Jackson, "DP flow sensor using optical fiber Bragg grating," Sens. Actuators A, Phys. **92**, 102–108 (2001).
7. X. Y. Fang and M. S. Cao, "Theoretical analysis of 2D laser angle sensor and several design parameters," Opt. Laser Technol. **34**, 225–229 (2002).
8. B. O. Guan, H. Y. Tam, and S. Y. Liu, "Temperature-independent fiber Bragg grating tilt sensor," IEEE Photon. Technol. Lett. **16**, 224–226 (2004).
9. X. Dong, C. Zhan, K. Hu, P. Shum, and C. C. Chan, "Temperature-insensitive tilt sensor with strain-chirped fiber Bragg gratings," IEEE Photon. Technol. Lett. **17**, 2394–2396 (2005).
10. H. J. Chen, L. Wang, and W. F. Liu, "Temperature-insensitive fiber Bragg grating tilt sensor," Appl. Opt. **47**, 556–560 (2008).
11. H. Bao, X. Dong, C. Zhao, L. Shao, C. C. Chan, and P. Shun, "Temperature-insensitive FBG tilt sensor with a large dynamic range," Opt. Commun. **283**, 968–970 (2010).
12. S. He, X. Dong, K. Ni, Y. Jin, C. C. Chan, and P. Shum, "Temperature-insensitive 2D tilt sensor with three fiber Bragg gratings," Meas. Sci. Technol. **21**, 025203 (2010).
13. K. Ni, X. Dong, Y. Jin, and H. Xu, "Temperature-independent fiber Bragg gratings tilt sensor," Microw. Opt. Technol. Lett. **52**, 2250–2252 (2010).
14. H. Y. Au, S. K. Khijwania, H. Y. Fu, W. H. Chung, and H. Y. Tam, "Temperature-insensitive Fiber Bragg gratings based tilt sensor with large dynamic range," J. Lightwave Technol. **29**, 1714–1720 (2011).